[14]H. S. Taylor, G. V. Nazaroff, and A. Golebiewski, J. Chem. Phys. 45, 2872 (1966).
[15]I. Eliezier, H. S. Taylor, and J. K. Williams, J. Chem. Phys. 47, 2165 (1967).
[16]R. H. Ritchie and J. E. Turner, Z. Physik 200, 259 (1967).
[17]L. M. Chanin, A. V. Phelps, and M. A. Biondi, Phys. Rev. 128, 219 (1962).
[18]Although the lifetimes of the known molecular resonance states are very short, it can be said that they are definitely longer than the duration of an ordinary elastic scattering collision of an electron and a molecule, which is in the order of 10^{-15} sec for thermal electrons. Hence it is not absurd to talk of electron trapping in connection with resonance scattering.
[19]The lifetime of this state is an estimated 10^{-14} sec; see Ref. 15. Hence an assumed mean cross section of 3×10^{-17} cm^2 for this state at $\bar{\epsilon}=1$ eV would yield $(\nu\tau)_1 = 0.6\times 10^{-6}$Torr^{-1}, in agreement with the experiment.
[20]D. J. Kouri, J. Chem. Phys. 45, 154 (1966).
[21]G. Herzberg, Spectra of Diatomic Molecules (D. van Nostrand Co., Inc., Princeton, 1950).
[22]A rigorous derivation requires one continuity equation for the free electrons, and one for each trapping state, with different lifetimes τ_1, τ_2, ..., etc. (see the appendix).
[23]D. E. Golden, Phys. Rev. Letters 17, 847 (1966).
[24]A. Watanabe and H. L. Welsh, Phys. Rev. Letters 13, 810 (1964).
[25]N. Bernardes and H. Primakoff, J. Chem. Phys. 30, 691 (1959).
[26]R. G. Gordon and J. K. Cashion, J. Chem. Phys. 44, 1190 (1966).
[27]D. E. Stogryn and J. O. Hirschfelder, J. Chem. Phys. 31, 1531 (1959); 33, 942 (1960).
[28]Joseph Hirschfelder, Charles Curtiss, and R. Bird, Molecular Theory of Gases and Liquids (John Wiley & Sons, Inc., New York, 1954) and Natl. Bur. Std. (U. S.), Circ. No. 564 (1955).
[29]T. A. Milne and F. T. Greene, J. Chem. Phys. 47, 3668 (1967).
[30]B. Kivel, Phys. Rev. 116, 926 (1959).
[31]T. F. O'Malley, Phys. Rev. 130, 1020 (1963).
[32]E. K. Müller, Z. Angew. Physik 21, 475 (1966).

Dissociative Attachment in CO and NO†

P. J. Chantry
Westinghouse Research Laboratories, Pittsburgh, Pennsylvania 15235
(Received 18 March 1968)

The electron energy dependences of the cross sections and of the ion kinetic energy distributions have been measured for O^- production from CO and NO. The present apparatus permits total collection measurements as well as kinetic energy analysis and mass identification of the ions produced. It is shown that in CO two reactions contribute to the single peak in the cross section, whereby carbon atoms are produced in their ground state and in their first excited state (^1D) respectively. The first reaction is predominant, and known from previous work to have a peak cross section of 2.0×10^{-19} cm^2. Normalized to this, the second reaction is shown to have a peak cross section of 9.5×10^{-21} cm^2. In NO it is shown that O^- production proceeds exclusively through the reaction $e+NO\rightarrow O^-+N^*$ where N* is the first excited state (^2D). No O^- ions are observed corresponding to the formation of ground state N. Nor is there any evidence for the production of the second excited state of nitrogen, N(^2P), postulated by Dorman to account for the structure in the attachment cross section.

INTRODUCTION

In two previous publications,[1,2] Chantry and Schulz have discussed in some detail the problems attending the experimental determination of the energetics of dissociative attachment reactions using electron beams, and the extent to which these problems are alleviated by making suitable direct observations of the ion kinetic-energy distributions as a function of electron energy. The superiority of such a technique over earlier techniques involving retarding potential analysis of the ion energies was demonstrated in Ref. 2 (hereafter referred to as CS) in a study of O^- production from O_2. The purpose of the present paper is to report the results of similar measurements on the reactions

$$e+CO\rightarrow O^-+C, \quad (1)$$

and

$$e+NO\rightarrow O^-+N. \quad (2)$$

These reactions were first observed by Vaughan[3] and by Tate and Smith[4] and have been studied repeatedly[5] since that time. The present study of the reaction (1) was undertaken to establish that the threshold does indeed correspond to the accepted values of the dissociation energy D and of the electron affinity A. In such cases as this, where the cross section rises very sharply, probably vertically, to a maximum value at threshold, the determination of the true threshold from a measurement of the energy dependence of the cross section presents an unfolding problem which requires a detailed knowledge of the electron energy distribution used.[6] An alternative approach is to measure the most probable ion energy as a function of most probable electron energy over as wide a range as possible, and extrapolate the data in the theoretically expected linear manner to the threshold. This method, used in CS to study

O^- production from O_2, has the advantage of being relatively insensitive to the details of either the cross-section shape or the electron energy distribution. In the present work this technique has been applied successfully to a determination of the threshold in CO, and establishes also that two separate processes contribute to the total cross section for O^- production from this molecule. The presence of two such processes is easily detected by the present technique provided they involve separate dissociation limits, since in this case the dependence of the ion kinetic-energy peaks on electron energy forms two sets of data, giving two distinct extrapolated thresholds.

The present study of O^- production from NO was undertaken in order to obtain a better understanding of the energetics of the process, and thereby of the shape of the cross section. In a recent paper Hierl and Franklin[5] claim that the appearance potential for O^- from NO is 5.0 ± 0.1 eV, from which they conclude that the dissociation products are $O^- + N(^4S)$, i.e., ground state N, for which the theoretical onset is 5.0 eV. In contrast to this, however, there are eight other values[7] for the experimentally observed appearance potential available in the literature,[5] all of which lie between 7.0 eV and 7.5 eV. It would, therefore, appear that either Hierl and Franklin were observing a different process from that observed by all other workers, or their electron energy-scale calibration was in error by two or more volts. Since two[4,6] of the eight previous determinations were performed with total ion collection, the former conclusion is more difficult to accept than the latter; and one concludes that their identification of the states of the dissociation products rests on questionable[7] experimental evidence.

Whilst there is a certain degree of agreement between other previous workers as to the appearance potential of O^- from NO, there is a distinct lack of agreement as to the dissociation limit and the shape of the cross section. Of particular interest is the double peak structure in the cross section observed in the previous total collection experiments.[4,6] On the basis of mass spectrometric and ion retarding-potential analysis, Dorman[5] has recently suggested that the structure arises from two separate processes leading to two distinct dissociation limits $O^- + N^*(^2D)$ and $O^- + N^*(^2P)$. This proposal may be easily tested with the present technique. As we shall see, we are led to the conclusion that the second process proposed by Dorman does not take place.

In Sec. I of this paper, the question of the exact behavior of the kinetic energy distribution in the threshold region is discussed on the basis of the exact theoretical distribution derived in CS. We consider also the effects on the observed position of the peak to be expected from ion energy discrimination in the experimental system. In Sec. II, a description of the experimental technique is given, with particular emphasis on the problem of adequately calibrating the electron and ion energy scales. In Sec. III, the results are presented and analyzed so as to identify the reactions occurring. On the basis of these results, qualitative potential energy curves for the XY^{-*} state involved are presented in Sec. IV.

I. THEORY

It has been shown by CS that in the reaction[8]

$$e + XY \rightarrow X^- + Y^* \tag{3}$$

the ion X^- produced by electrons of energy V_e will have a kinetic energy distribution whose most probable energy is at E_0, defined as

$$E_0 = (1-\beta)[V_e - (D - A + E^*)], \tag{4}$$

where $\beta = m/M$, m and M being the masses of X^- and XY, respectively, D is the dissociation energy of XY, A is the electron affinity of X, and E^* is the excitation energy of Y^*. Therefore, if one measures the most probable ion energy as a function of electron energy V_e, one may analyze the data using Eq. (4). That is to say, one fits the data points with a straight line of slope $(1-\beta)$ and extrapolates, if necessary, to zero ion energy. The value of V_e at this intercept provides a determination of $(D - A + E^*)$, from which we may identify the state of excitation of the neutral fragment. As shown by CS, the appearance of the peak of the distribution (the most probable ion energy) at E_0, defined by Eq. (4), is conditional on satisfaction of the inequality $E_0 \gg \beta kT$. In the case of O^- from O_2 considered by CS this condition was well satisfied throughout the range of E_0 of interest. As will be seen, in the present work O^- is produced from CO and NO over a range of E_0 extending down to zero, where the condition $E_0 \gg \beta kT$ is obviously not satisfied. The exact behavior of the most probable ion energy in the threshold region is therefore of interest.

The most probable ion energy in the *observed* peak is also dependent, over the whole energy range, on the degree of energy discrimination present in the ion detection system. For the purpose of analysis this will be assumed to be of the form E^{-n}, in which case the shape of the observed energy distribution is determined by[9]

$$I_{MS}(E) = CE^{-n} e^{-E/\beta kT} \times \sinh(2E_0^{1/2} E^{1/2}/\beta kT), \tag{5}$$

where I_{MS} is the current of O^- detected by the mass spectrometer when the ion energy analyzer is tuned to transmit ions of initial energy E. C is a constant in that it is independent of E, this being the only aspect of it of interest to the present discussion. The position of the observed peak is given by equating to zero the differential of Eq. (5) with respect to E. For convenience we define the dimensionless energies

$$\alpha^2 = E/\beta kT \text{ and } \alpha_0^2 = E_0/\beta kT. \tag{6}$$

In terms of these, the position of the observed peak α_p^2 is given by one[10] of the roots of the equation

$$\alpha_0^2 = (\alpha + n/\alpha)^2 \tanh^2(2\alpha\alpha_0). \quad (7)$$

This may be solved numerically, allowing α_p^2 to be plotted as a function of α_0^2 for various choices of n. Fig. 1 shows four such curves, for $n = 0$, 0.5, 1, and 2. The broken parts of the curves correspond to minima in the distribution given by Eq. (3), which arise for $n \neq 0$,

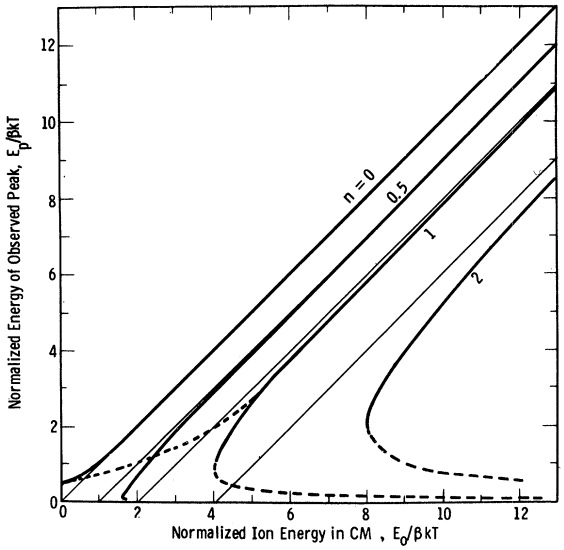

FIG. 1. The calculated position of the ion-current peak plotted as a function of E_0, defined by Eq. (4), showing the effect of ion energy discrimination of the form E^{-n}. The heavy curves are plots of Eq. (7), the broken portions corresponding to minima in the observed distribution. The straight lines of unit slope are the high-energy asymptotes. The dotted curve is a qualitative representation of the behavior expected in a practical situation for the case $n = 1$.

when there is always a corresponding peak at $E = 0$. From a practical point of view, however, one does not expect to see such a minimum for small values of n; first, because the E^{-n} weighting factor cannot be expected to apply for very small E, and second, because the finite resolution available experimentally will not allow the minimum to be traced out. Provided an adequate ion-extraction field is applied, one expects the collection efficiency to be independent of E in the region of $E = 0$, so that as E_0 is decreased the position of the observed peak will first follow the curve appropriate to the value of n involved, but will then cross over in a smooth manner to the $n = 0$ curve as E_0 approaches zero. Behavior of this type is qualitatively represented by the dotted curve for the case of $n = 1$.

We note that, in the case of no energy discrimination ($n = 0$), as E_0 approaches zero, the most probable energy approaches the value $\beta kT/2$, corresponding to the Maxwellian distribution of velocities of the target molecules. Thus, in the limit of $E_0 = 0$ the ions are produced with a temperature reduced from that of the target molecules by the factor β, since they have the same velocity distribution but a mass reduced by this factor.

The near-threshold behavior of the observed energy distribution, represented in Fig. 1, may be put in perspective by noting that the instrumental energy resolution in the present experiment corresponds to a "window" of width at half maximum of approximately 0.1 eV. This corresponds, at room temperature and for these particular gases, to approximately $7\beta kT$. Thus we cannot expect to resolve any structure imposed in this region by the energy discrimination. We note, however, that for small n and energies greater than a few βkT the observed most probable energy appears $2n\beta kT$ below the true value.[11] As will be shown, in the present experiments n is always less than 1, so that this displacement may always be expected to be less than 0.03 eV.

II. EXPERIMENT

The measurements to be presented were performed using the apparatus shown in Fig. 2. The electrode system is a modification of that used by CS, wherein a full description of the apparatus and its mode of operation may be found. The modifications are described in some detail below, with a brief account of the essential features of the technique.

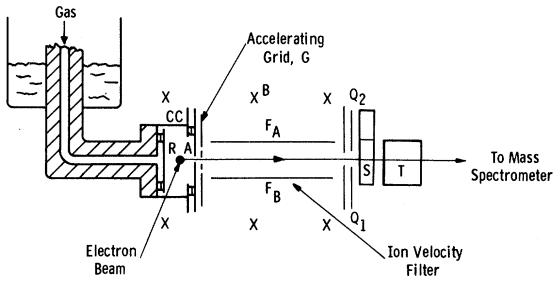

FIG. 2. Diagram of the modified "split" collision chamber and the ion velocity (Wien) filter. See text and CS.

The gas under study is admitted to the collision chamber through a heavy copper capillary, which also serves to support the electrode system within the vacuum envelope. When required, the part of the copper capillary external to the main vacuum envelope may be heated or cooled, providing a corresponding change in the temperature of the gas entering the collision chamber. This feature was not used in the present work; all measurements were carried out with the gas at room temperature. The cylindrical electron beam is collimated by an electrode system which permits the use of the retarding potential-difference (R. P. D.) technique[12] for reducing the effective energy spread of the electron beam. The beam is aligned by the magnetic field indicated by the crosses in Fig. 2 and travels perpendicular to the diagram along an essentially equipotential surface within the collision chamber. This is achieved by arranging that the ion-

extraction field imposed between the repeller (R) and attractor (A) electrodes be symmetrical with respect to the potential of the main collision chamber box (CC).

Under the influence of the ion-extraction field, the majority[13] of negative ions formed within the collision chamber reach the attractor. Of these a small sample passes through the narrow (0.05×1.4 cm) slit in the attractor, which provides essentially a line source of ions entering the Wien filter.

The function of the accelerating grid G is to transfer the ions from the exit slit in the attractor electrode into the region between the condenser plates F_A and F_B with minimum perturbation of their paths by the magnetic field. Within the region between the plates F_A and F_B, their trajectories are controlled by the crossed electric (E) and magnetic (B) fields, and under the conditions of operation will pass through the exit slit only if their axial velocity v in the crossed field region satisfies the condition $v = E/B$.

As might be expected, the ion current transmitted by the system increases with increasing accelerating voltage applied to the grid G. The application of more than approximately 5 V to the grid was found, however, to cause serious deterioration of the energy resolution of the filter, presumably due to penetration of the grid potential into the analysis region between plates F_A and F_B. The optimum choice of grid potential was found to be approximately 3 V accelerating with respect to the attractor electrode.

On leaving the Wien filter, the ions enter the mass spectrometer through a series of electrodes (Q, S, T). The purpose and mode of operation of these electrodes has been previously described in CS. They are used in an identical fashion in the present work. Ions transmitted by the mass-spectrometer are detected by a secondary electron multiplier whose output is coupled to a vibrating-reed electrometer.

Total Collection Measurements

In a conventional mass-spectrometer ion source, such as that used initially by CS, it is possible to make measurements of the total ion current produced in the source by collecting the ions on what is normally the repeller electrode. To do so, however, requires that the polarity of this electrode be reversed from that used when operating the mass-analyzer, with a consequent unknown shift in the electron energy scale. Moreover, the asymmetry of the ion-extraction field in such a geometry gives rise to variations of potential along the electron beam of the same order as the voltage applied between the collision chamber and the repeller. The advantages of the present design of collision chamber have discussed in some detail in CS. Of particular value in the present work is that it allows one to make measurements of the total ion current reaching the attractor or the repeller. Thus, for the measurement of total negative or positive ion currents these electrodes may be held at the same potentials as are applied for operation of the collision chamber with the Wien filter and mass spectrometer, in which case the same electron energy scale applies to both types of measurements. Moreover, the extraction field may be so arranged that the electron beam traverses the collision chamber along an essentially equipotential surface,[14] the energy resolution being degraded only to the extent of the potential variation transverse to the beam imposed by the ion-extraction field.

The term "total" has been applied somewhat loosely to the measurements carried out with the present system. Because there are no guard plates, the current collected on either the repeller or attractor cannot be expected to comprise all the ions produced in a well defined region, even with a large extraction field. In deciding whether or not the extraction field is adequate, the criterion adopted is not the usual one of current saturation,[6] but rather requires only that the shape of the cross section as a function of the electron energy be insensitive to further increases in the extraction field. In general, one uses the minimum adequate extraction field in order to preserve the best possible electron energy resolution.

The present design of collision chamber was chosen for its properties as a mass-spectrometer ion source. It is not ideal for total-collection measurements in that *absolute* determinations of cross sections cannot be made. The *shapes* of cross sections can, however, be accurately determined, as shown by the measurements of O^- production from O_2 reported in CS, and of O^- from CO reported here in Sec. III.

Electron Energy-Scale Calibration

The electron energy scales used in plotting the results of the present work have been chosen to correspond as closely as possible to the most probable electron energy of the distribution used. In the work on CO, it was found that the magnitude of the cross section for the reaction (1) is so small that, for the measurement of ion kinetic-energy distributions, the retarding potential-difference technique could not be usefully employed at electron energies other than near the peak of the cross section. For the sake of consistency all the ion energy distributions measured in CO were taken using a retarded distribution, that is, one in which the low-energy part of the distribution has been removed by the retarding electrode of the R. P. D. gun. The electron energy scale used for the data taken with this distribution (Figs. 4(b) and 5) was calibrated by relating the onset of positive ions (CO^+) measured at the repeller to the known ionization potential (14.0 eV).

In the present work we require a scale corresponding to the most probable electron energy. This is obtained from the CO^+ appearance-potential curve, which is known to be linear immediately above threshold,[15] by correcting the electron accelerating voltage scale so that the true appearance potential (14.0 eV) occurs midway between the linearly extrapolated

threshold and the energy at which the linear behavior is established. These points correspond respectively to the average energy and to the minimum energy of the distribution. It is assumed that the most probable energy lies close to the mean of these two.[16]

The total measurements of negative ion current reaching the attractor, plotted in Fig. 4(a), were taken using the R. P. D. technique. The energy scale in this case was that given by the linearly extrapolated positive-ion appearance curve measured on the repeller using the same R. P. D. distribution.

In the work on NO, the cross section is sufficiently large, so that it was possible to use the R. P. D. technique for the measurements of ion energy distributions as well as for the total measurements. The electron energy scale in this case was calibrated in two ways: first, from the retarding curve of the difference electron-energy distribution, and second, from a positive-ion appearance potential. In this case, the NO^+ appearance curve was not used, its shape being distinctly nonlinear near threshold[17] and, therefore, unsuitable for this purpose. The following procedure was adopted. Using a mixture of NO and Xe, and with the field between the repeller and attractor arranged to extract positive ions into the mass spectrometer, curves were taken of the total negative ion current reaching the repeller, and the appearance curve for Xe^+ observed through the mass spectrometer. The latter is known[18] to be linear for approximately 1 eV above threshold, and thus is useful for calibration purposes. Knowing the position of the total negative-ion curve on the electron energy scale calibrated in the above manner, the polarity of the ion-extraction field was returned to normal and the total negative-ion curve measured at the attractor used thereafter to calibrate the electron energy scale.

Finally, having obtained the data for CO and NO separately, mixtures of these gases were employed to obtain a set of data representing essentially a composite of Figs. 5 and 9 discussed below. No attempt was made in this case to calibrate the electron energy scale absolutely. The measurements, however, provide a direct determination of the difference between the onsets of the three reactions involved. Excellent agreement was found with the values expected on the basis of the measurements made in the separate gases. In particular, the onset for the NO reaction was found to be 2.20 eV below that for the first reaction in CO.

Measurement of Ion Energy Distributions

As described in more detail in CS, the ion energy distribution produced at a given electron energy is scanned by sweeping the accelerating voltage between the Wien-filter electrode system (F_A, F_B, F, Q, S) and the collision chamber box (CC) over the appropriate range. The ion energy scale is calibrated by noting the ion accelerating voltage at which ions of initially zero (i.e., thermal) energy are transmitted by the filter. In the present studies such ions were found to be directly available at the thresholds of the dissociative attachment processes.

The shape of the cross section in the threshold region for O^- production from CO, as determined by the measurements of total ion current, was found to be essentially identical to the corresponding electron retarding curve irrespective of the electron energy distribution used. Thus, the cross section must approximate a step function over a range of energy comparable to the width of the electron energy distributions used. A vertical onset for a dissociative-attachment cross section indicates that the negative-molecular-ion potential-energy curve involved rises above the dissociation limit somewhere within the Franck-Condon region,[19] in which case the ions produced at threshold have only thermal velocities. The observations using the Wien filter are consistent with this; for electron energies nominally below the threshold the ion current peak always occurs at the same ion accelerating voltage, with the width of the peaks corresponding to the known instrumental width. The ion accelerating voltage at which the peaks appeared in this range of nominal electron energy was, therefore, used as the zero[20] of the corresponding ion kinetic-energy scale.

Somewhat surprisingly, a similar situation[21] was found to arise in NO, and the same procedure was adopted to calibrate the ion energy scale. The validity of these procedures is strongly supported by the observation that, using a mixture of CO and NO, the ion energy peaks observed in the regions of electron energy below the nominal thresholds were identical in position and shape.

Ion Kinetic-Energy Discrimination

As discussed in Sec. I, measurements of the ion kinetic energy as a function of electron energy will be subject to error, if there is serious ion energy discrimination present in the overall transmission of the Wien-filter mass-spectrometer system. In the present work the energy dependence of the overall transmission efficiency, $f(E)$, has been checked in the following way. At a given electron energy, and with the filter tuned to the peak E_0, of the ion energy distribution, the O^- current I_{MS} detected by the mass spectrometer is proportional to[22] $\sigma(V_e)$ $E_0^{-1/2} f(E_0)$, where $\sigma(V_e)$ is the dissociative-attachment cross section at energy V_e. The "total" current, I_T, collected on the attractor is proportional simply to $\sigma(V_e)$. Hence, $f(E_0)$ $\propto I_{MS} E_0^{1/2}/I_T$. Thus, a plot of this ratio as a function of E_0 will reveal the form of $f(E)$. Samples of such data are shown in Fig. 3. In order to apply the theoretical analysis of Sec. I, we fit to the data functions of the form E^{-n}. In these cases[23] $n \leq 0.6$, and, in general, values of $n < 1$ are found for the present system. In Sec. I it was shown that the observed most-probable ion energy will appear at $E_0 - 2n\beta kT$ for energies

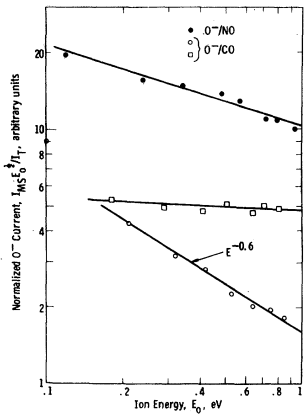

FIG. 3. The dependence of the transmission efficiency of the Wien-filter mass-spectrometer system on the initial-ion kinetic energy. The three sets of data were obtained in separate runs with slightly different tuning conditions of the filter.

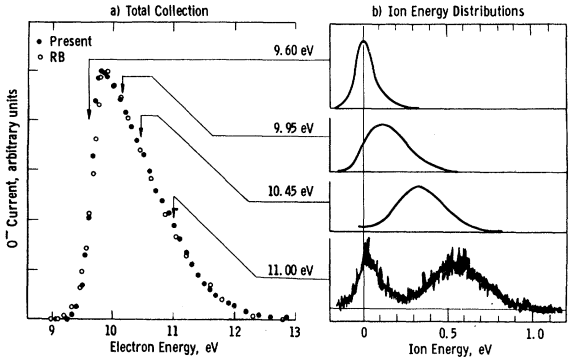

FIG. 4. The cross section and ion energy distributions for O^- production from CO. In (a) the total current collected by the attractor is plotted as a function of electron energy, taken using the R.P.D. technique. Also shown is the R. P. D. data of Rapp and Briglia (Ref. 6). The two sets of data have been normalized at 10.5 eV. In (b) ion energy distributions observed with the Wien filter at four different electron energies are shown.

other than very close to threshold. The corresponding extrapolated threshold will then be too high by $2n\beta kT/(1-\beta)$, which for $n = 0.6$ amounts to approximately 0.04 eV for the present cases. This is less than the over-all confidence limits involved in the energy scale calibrations, and no attempt has been made to apply a systematic correction for it. We note, however, that the experimentally determined thresholds presented in the next section do exceed the theoretical values, by 0.08 and 0.07 eV in the case of CO and by 0.08 eV in the case of NO, suggesting that a systematic error is present, quite possibly due, in part, to the above effect.

III. RESULTS

In the present work two types of measurement have been made. The total difference current[24] reaching the attractor has been recorded as a function of electron energy, and under suitable conditions of extraction voltage is believed to provide the shape of the dissociative-attachment cross section. Secondly, the ion energy distributions of the mass-analyzed O^- sample entering the Wien filter have been recorded at various electron energies. These results are presented below, in turn, for the gases studied, CO and NO.

O^- from CO

The shape of the cross section for negative ion production in CO is shown in Fig. 4(a). The present data shown were taken with an ion-extraction field of 0.8 V/cm. Increasing the extraction field to three times this value gave a curve identical in shape to that shown, indicating that the ion-collection efficiency is not a function of initial ion kinetic-energy in this case. Also shown are the R. P. D. data of Rapp and Briglia,[6] taken in a Tate and Smith apparatus. The curves have been normalized in magnitude at 10.5 eV, where any difference in electron energy distributions may be assumed not to affect the shape. The two shapes are in excellent agreement, the slight discrepancies in the threshold region suggesting that the electron energy resolution is a little better for the present data. As pointed out by Rapp and Briglia, the actual shape observed between the apparent threshold and the apparent peak of the cross section is determined by the electron distribution. Assuming that the cross section behaves as a step function over this small range, and that the electron energy scale corresponds to the most probable electron energy, the true threshold for the process will correspond to the steepest part of the observed onset. For the present data, this occurs at 9.65 ± 0.05 eV, in excellent agreement with the value one calculates from the accepted values of D (11.09 eV)[25] and A (1.47),[26] i.e., 9.62 eV.

As discussed in Sec. I, an alternative method of finding the energy threshold for a dissociative-attachment process is to plot the most probable ion energy as a function of electron energy, and fit to the data a straight line of the appropriate slope. To this end, ion energy distributions were measured at various settings of the electron energy, a sample of such data obtained in CO being shown in Fig. 4(b). The curves shown are smooth tracings through x-y recordings of the electrometer output as a function of ion accelerating voltage.[27] As explained in the previous section, the peaks observed at and below the true threshold reflect the instrumental width of the Wien filter, the zero of the ion energy scale therefore corresponding to the position of the peak in this region of electron accelerating voltage. An indication of the noise present on the original x-y recordings is given on the lowest curve shown. In general, because of the changing cross section, curves taken at electron energies below this particular value (11.0 eV) are less noisy than shown; those taken above are more noisy. It is seen that at 11.0 eV a second peak of near-zero kinetic energy has appeared in the ion energy spectrum. At higher electron energies the two peaks appear with essentially the same separation, both being at appropriately higher ion energies.

The systematic analysis of data of this type is shown in Fig. 5, where the position of the ion energy peak, or peaks, is plotted as a function of the electron energy. The straight lines through the two sets of points have been drawn with a slope of $\frac{12}{28}$, as prescribed by the theory presented in Sec. I. The fit to the more extensive set of points is seen to be good, providing a well defined value of 9.70 ± 0.1 eV for the energy threshold. The limits of error placed on this value reflect mostly the limits of confidence in the energy scale calibrations, rather than scatter in the data points. For this reason the threshold for the second process observed is quoted with the same limits of error, 10.95 ± 0.10 eV, in spite of the fact that the data points are less extensive and show more scatter.

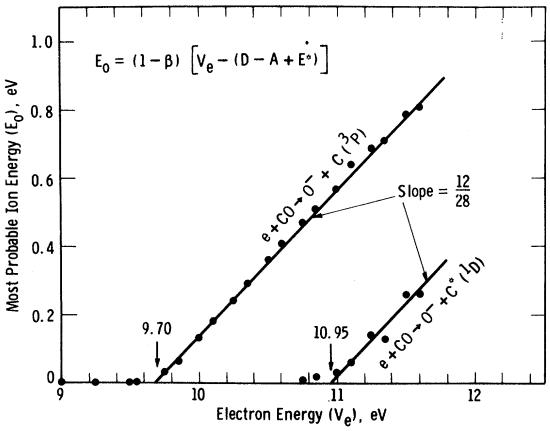

FIG. 5. Measured values of the most probable O^- ion energy plotted as a function of electron energy for CO. The straight lines are drawn with the theoretical slope of $(1-\beta) = \frac{12}{28}$. Within experimental error, the thresholds (9.70 and 10.95 eV) are consistent with the reactions indicated.

The energy thresholds, 9.70 ± 0.10 and 10.95 ± 0.10 eV, determined by Fig. 5, are within experimental error those calculated for the processes

$$e + CO \rightarrow O^- + C(^3P), \text{ at } 9.62 \text{ eV} \quad (8)$$

$$e + CO \rightarrow O^- + C^*(^1D), \text{ at } 10.88 \text{ eV} \quad (9)$$

from the accepted values of the dissociation energy[25] of CO ($D = 11.09$ eV), of the affinity[26] of O ($A = 1.465$ eV), and of the excitation energy[28] of $C^*(^1D)$ ($E^* = 1.26$ eV). We therefore conclude that production of O^- from CO occurs by way of the reactions (8) and (9) above.[29]

So far as can be determined, the cross section for the second process has a shape similar to that for the first. An alternative method of determining the separation of the two thresholds is to set the Wien filter to transmit ions of a particular energy and to record the negative ion current as a function of electron energy. The sharpest peaks are obtained, understandably, if one observes ions of zero initial energy. Such a plot is shown in Fig. 6. The separation of the peaks, 1.22 eV, is in excellent agreement with the thresholds obtained from Fig. 5.

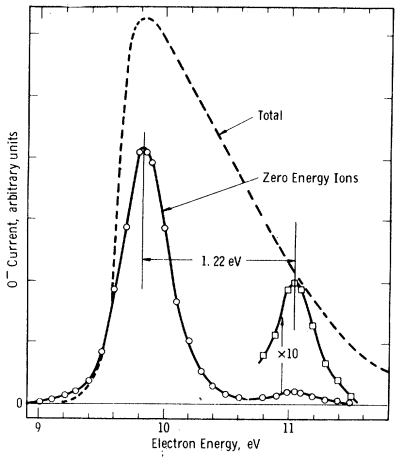

FIG. 6. Electron energy dependence of the O^- current observed in CO with the Wien filter tuned to zero initial ion energy. The separation of the two peaks corresponds to the excitation energy of $C^*(^1D)$ produced by the second process. The total current collected by the attractor is shown for comparison. Their relative magnitudes are chosen for convenience of presentation, and have no other significance.

The relative magnitudes of the cross sections for the two processes at their maxima has been estimated by plotting the heights of the two peaks shown in Fig. 6 as a function of CO pressure. These data are shown in Fig. 7, which serves to show that both processes are first order in pressure,[30] as expected for dissociative attachment. The lines of unit slope drawn through the data points are separated by a factor of 21. The cross section determined by Rapp and Briglia[6] has a maximum value of 2.0×10^{-19} cm^2. We therefore conclude that the second process observed in the present work has a maximum cross section of 9.5×10^{-21} cm^2.

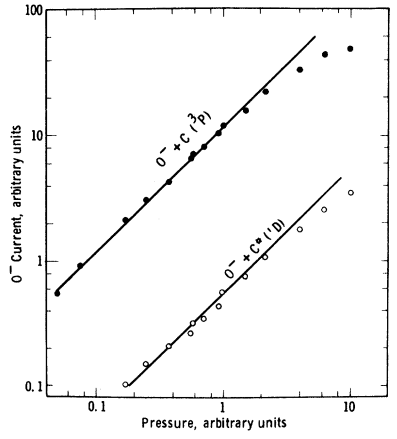

FIG. 7. Pressure dependences and relative magnitudes of the O^- currents produced at the peaks of the two processes in CO. These data are taken with the Wien filter tuned for zero-energy ions. The lines through the data points have unit slope and are separated by a factor of 21. Unity on the pressure scale corresponds approximately to 3×10^{-4} Torr.

O^- from NO

The "total" measurements of the O^- current reaching the attractor in the case of NO show a significant dependence of the shape of the cross section on the extraction field, it being apparently more difficult to collect the ions formed at the higher electron energies. This effect is shown in Fig. 8, where the shapes observed in the present work at two values of the ion-extraction

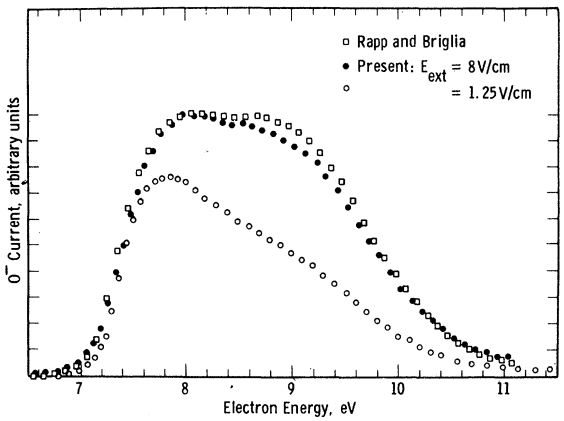

FIG. 8. The "total" ion current collected by the attractor in NO plotted as a function of electron energy for two values of the ion-extraction field. For comparison, the data of Rapp and Briglia (Ref. 6) are also shown, shifted to higher energies by 0.05 eV in order to match the leading and trailing edges with the present data taken with an extraction field of 8 V/cm. The latter curve is normalized in magnitude to the data of Rapp and Briglia at the peak. The relative magnitudes of the two present curves shown is that observed experimentally.

field are plotted, together with the result of Rapp and Briglia.[6] Increasing the extraction field to 16 V/cm changed the shape from that observed using 8 V/cm only in that, at the higher extraction field, the negative ion peak is superimposed on a background current, and has a smaller apparent slope at onset. These effects are due, respectively, to the collection of scattered electrons and to the broadening of the electron energy by the high transverse field. Some evidence of this latter effect is present in the data taken at 8 V/cm. The relative magnitudes of the two humps in the attachment peak were not changed by the higher extraction field of 16 V/cm. It is, therefore, believed that the data taken with an extraction field of 8 V/cm do not suffer from serious discrimination against higher energy ions (in contrast to the data taken at 1.25 V/cm). In Fig. 8, the present data obtained using 8 V/cm and the data of Rapp and Briglia have been normalized in magnitude to give the same maximum cross section. The same normalization factor has been applied to both sets of present data, so that the relative magnitude of the currents observed using the two different extraction voltages has been preserved.

The data points of Rapp and Briglia have been shifted[31] to higher energies by 0.05 eV in order to match the leading and trailing edges of their curve to the present data taken using 8 V/cm. The over-all agreement is then seen to be good, except for some discrepancy in the region of the second hump. One is tempted to ascribe this to some remaining discrimination in the present measurement against ions of higher initial kinetic energies. However, if this were the case, one would expect that the present results would fall consistently below the data of Rapp and Briglia as one increased the electron energy. This is not the case at energies above 10.2 eV. No explanation of the discrepancy can be offered at this time.

The exact shape of the cross section in the immediate threshold region is more difficult to interpret from the measured shape for NO than in the case of CO. If a broad electron energy distribution is used, the shape observed follows very closely the shape of the electron-current retarding curve, showing that the cross section rises very steeply, possibly vertically at threshold, to near its maximum value. Using a narrower (R. P. D.) electron energy distribution gave a steeper total-current curve in the threshold region, but the correspondence of shape to the electron retarding curve was not preserved with the narrower electron energy distribution. This observation, together with the observation of zero energy ions over a range of electron energies nominally below the threshold, similar to those observed in CO, suggest that the cross section rises vertically at threshold to some fraction, say one half, of its maximum value, and then rises steeply but with finite slope to very near its maximum value.

The O^- ion kinetic-energy distributions produced from NO behave as a function of electron energy in a similar fashion to those produced by the reaction (8) in CO. That is to say, at nominal electron energies below the true threshold the ion kinetic-energy distribution has a width determined by the "window" of the Wien filter. With increasing energy the distribution shifts to higher energies and broadens, as predicted by theory. In contrast to CO, however, and in contradiction to the proposal of Dorman[5] that two separate dissociation limits of $O^- + N^*$ are involved in the process, a second peak does not appear in the ion kinetic-energy spectrum. This behavior is shown in Fig. 9, where the position of the peak of the ion energy distribution is plotted as a function of electron energy. It is seen that all the data points may be fitted with a single straight line; the one shown having been drawn with the theoretically predicted slope of 14/30. The energy threshold, 7.50 ± 0.10 eV, so determined is in excellent agreement with that calculated (7.42 eV) for the process

$$e + NO \rightarrow O^- + N^*(^2D) \qquad (10)$$

from the accepted values of the dissociation energy[25] of NO ($D = 6.506$ eV), of the affinity[26] of O ($A = 1.465$ eV) and of the excitation energy[32] of N^* (^2D) ($E^* = 2.383$ eV). We therefore conclude

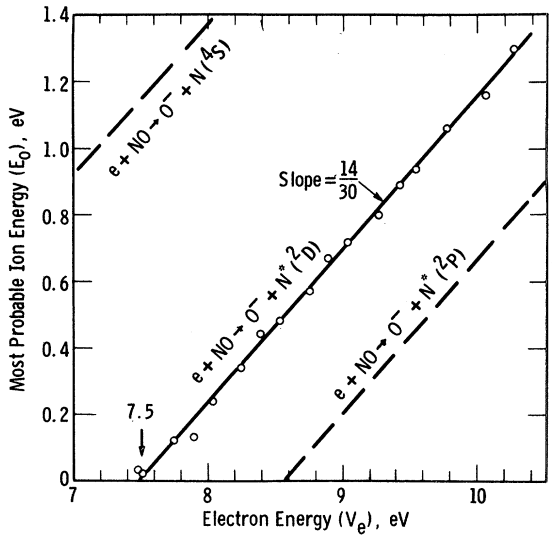

FIG. 9. The measured values of the most probable O^- ion energy from NO plotted as a function of electron energy. The straight line through the data points has the theoretical slope $\frac{14}{30}$, and intercepts the abscissa at 7.5 ± 0.1 eV, consistent with the reaction indicated. The two broken lines indicate the positions in which peaks would be found, if the reactions indicated occurred. No such peaks were observed.

that O^- production from NO occurs exclusively by way of the reaction (10) above.

IV. POTENTIAL ENERGY CURVES

Because of the resonant nature of the dissociative-attachment process, the shape of the cross section as a function of electron energy serves as an approximate guide to the position and slope of the negative-molecular-ion potential-energy curve in the Franck-Condon region. Theoretical work[33,34,35] on this subject has shown that the dissociative-attachment cross section may, with certain restrictions,[35] be written[34] as

$$\sigma(E) \propto (\Gamma_{\bar{a}}/EV')|\chi(E)|^2 e^{-\rho(E)} \qquad (11)$$

where E is the electron energy, $\Gamma_{\bar{a}}$ is the entrance width,[36] V' is the slope of the intermediate XY^{-*} potential energy curve, $\chi(E)$ is essentially the initial vibrational wave function written in terms of the electron energy,[37] and $e^{-\rho(E)}$ is the probability that the XY^{-*} state does not decay through autodetachment before dissociating into stable fragments $X^- + Y$.

The reflection method[38] for the construction of potential energy curves, used frequently in the past, draws the XY^{-*} potential energy curve such that the square of the initial vibrational wave function, when reflected in the XY^{-*} potential energy curve, reproduces the shape of the cross section on the energetically allowed region of the energy axis. In terms of the above equation, this is essentially equivalent to replacing the factor $(\Gamma_{\bar{a}}/V')\, e^{-\rho(E)}$ by a constant. In some cases, other evidence[39,40] has permitted estimates of the energy-dependent effects of these factors, and allowed semiempirical derivations[41,42] of the salient features of the XY^{-*} potential energy curves, that is, their positions *and widths* as functions of internuclear separation. In these cases the influence of the survival probability $e^{-\rho(E)}$ on the observed shape of the cross section has been shown to be very strong.[43] The influence of the factor $\Gamma_{\bar{a}}/EV'$ is less severe. The slope V' of the XY^{-*} potential energy curve will generally not vary strongly in the Franck-Condon region, and may be regarded as constant relative to other factors. The factor E^{-1} may obviously be taken into account directly in attempting to relate the observed shape to the position and slope of the potential energy curve. However, the entrance width $\Gamma_{\bar{a}}$ is likely to increase with decreasing internuclear separation R, thereby increasing with E, and it may be a better approximation to assume that $\Gamma_{\bar{a}}/E$ is only weakly dependent on E.

We may conclude from the foregoing discussion that the position and slope of the XY^{-*} potential energy curve in the Franck-Condon region can only be determined *very approximately* from the shape of the attachment cross section measured at one temperature. Thus, the XY^{-*} curves[44] presented in Figs. 10 and 11 must be regarded as essentially qualitative. Nevertheless, such curves provide a useful means of presenting the conclusions to be drawn from such work as the present, and provide a basis for more sophisticated determinations which hopefully will become possible in the future.

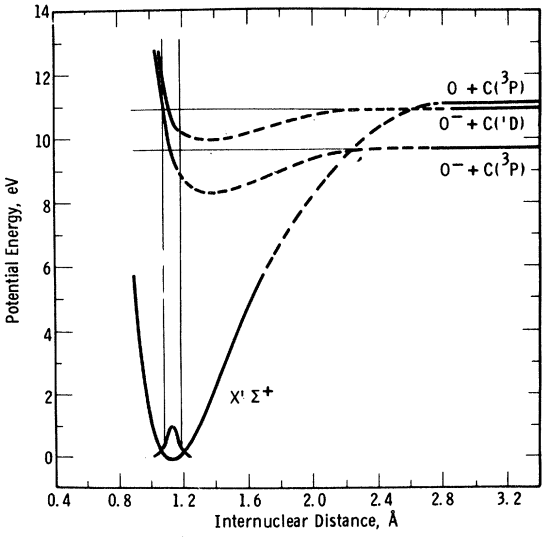

FIG. 10. Qualitative potential energy curves for the CO^{-*} states involved in dissociative attachment. The positions and depths of the minima are speculative, and are drawn in only to indicate the respective dissociation limits of the two curves.

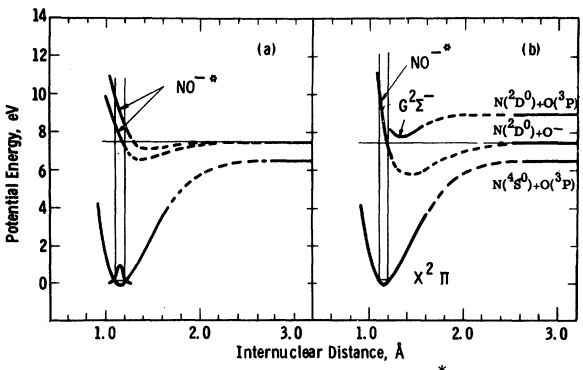

FIG 11. Potential energy curves of NO^{-*} consistent with two alternative interpretations of dissociative attachment in NO. In (a) the structure has been assumed to arise from two separate reactions involving separate NO^{-*} states. In (b) it is assumed that only one state is involved, the structure in the cross section being due to survival-probability effects. The neutral $G^2\Sigma^-$ state is an example of the many neutral states crossing the Franck-Condon region in this energy range. The positions and depths of the minima shown for the NO^{-*} curves are speculative and are drawn in only to indicate the dissociation limit.

The present work on O^- production from CO has shown that two distinct states of CO^{-*} are involved, leading to the two distinct dissociation limits, $O^- + C(^3P)$ and $O^- + C^*(^1D)$. The fact that both processes have, so far as can be determined, vertical onsets and maximum cross sections at onset suggests that the potential energy curves involved rise above their respective dissociation limits in the Franck-Condon region, and at internuclear separations less[45] than the equilibrium value for the initial ground vibrational state. The state dissociating to $O^- + C^*(^1D)$ has been drawn with this crossing point at a smaller internuclear separation than that for the state leading to ground state fragments, in order to be consistent with the relative magnitudes of the observed cross sections and their extent in electron energy.

In order to account for the width of the cross-section peak, one requires that, above the dissociation limit, the potential energy curve stays in the Franck-Condon region over an appropriate range of energy. Clearly the choice of slope depends on the choice of internuclear separation at which the curve rises above the dissociation limit. Thus the combination chosen in Fig. 10 is not unique.

The present measurements have shown that in the production of O^- from NO only one dissociation limit, $O^- + N^*(^2D)$, is involved. Thus it is not obvious that the two peaks in the cross section should be interpreted as arising from capture to two separate states of NO^-. The present work does not rule out this possibility, however, but shows that if two such states are involved, both go to the same dissociation limit.

We shall consider two possible explanations[46] of the structure in the cross section: (a) The cross-section curve consists of two separate but incompletely resolved bell-shaped curves, arising from two separate NO^- potential energy curves, both having the same dissociation limit. Alternatively, (b), there is only one NO^{-*} potential energy curve involved, the structure being imposed on what is basically a single bell-shaped curve (with a low energy cutoff) by the energy dependence of the survival probability.[47]

The potential energy curves of NO^{-*} which are qualitatively consistent with the above alternative interpretations of the structure in the cross section are presented in Fig. 11(a) and (b). The lower curve in Fig. 11(a) and the single curve in Fig. 11(b) are shown rising above the dissociation limit just within the Franck-Condon region, to be consistent with the suggestion made in Sec. III that the cross section rises vertically at threshold to some fraction of its maximum value, rising steeply thereafter to very near its maximum value. The many neutral states[44] of NO in the region of 8 eV have not been shown for reasons of clarity.

Finally, it must be stressed that the XY^{-*} state potential energy curves presented in Figs. 10 and 11 are to be regarded only as qualitative.

V. CONCLUSIONS

The results of the present work allow the following conclusions to be drawn regarding the production of O^- from CO and NO.

(a) In CO, two reactions occur:

$$e + CO \rightarrow O^- + C(^3P),$$

and $e + CO \rightarrow O^- + C^*(^1D)$.

(b) The thresholds for these occur, within experimental error, at the theoretical values of 9.62 and 10.88 eV.

(c) The peak cross sections of these processes occur at or very close to thresholds, and differ in magnitude by a factor of 21. Thus, by normalizing to the known value of the first peak (2.0×10^{-19} cm^2), one concludes that the second has a value of 9.5×10^{-21} cm^2.

(d) In NO, only one reaction occurs:

$$e + NO \rightarrow O^- + N^*(^2D).$$

(e) The threshold for this occurs at the theoretical value of 7.42 eV.

(f) The double peak structure of the cross section in NO may or may not result from two separate processes involving two intermediate NO^{-*} states. If two such states are involved they are both associated with the same dissociation limit, $O^- + N^*(^2D)$.

ACKNOWLEDGMENTS

Much of the technical experience, without which the present work would not have been possible, was gained by the author during a period of collaboration with G. J. Schulz, now of Yale University. It is a pleasure also to acknowledge frequent discussions with A. V. Phelps and other members of the Atomic Physics Group at Westinghouse and also the technical assistance of W. M. Uhlig.

†This research was supported in part by the Advanced Research Projects Agency through the U. S. Office of Naval Research.

[1]P. J. Chantry and G. J. Schulz, Phys. Rev. Letters 12, 449 (1964).

[2]P. J. Chantry and G. J. Schulz, Phys. Rev. 156, 134 (1967).

[3]A. L. Vaughan, Phys. Rev. 38, 1687 (1931).

[4]J. T. Tate and P. T. Smith, Phys. Rev. 39, 270 (1932).

[5]For a recent bibliography, see L. J. Kieffer, Natl. Bur. Std. Misc. Publ. No. 289, 1967. In addition, see F. H. Dorman, J. Chem. Phys. 44, 3856 (1966) and P. M. Hierl and J. L. Franklin, J. Chem. Phys. 47, 3154 (1967).

[6]See, for example, D. Rapp and D. D. Briglia, J. Chem. Phys. 43, 1480 (1965).

[7]Hierl and Franklin quote none of the eight values available in the literature. They incorrectly attribute to Hagstrum [H. D. Hagstrum, Rev. Mod. Phys. 23, 185 (1951)] the value of 3.2 eV for the appearance potential. Hagstrum's measured appearance potential is in fact close to 7.4 eV, as clearly shown in his Fig. 19. As explained by Hagstrum in the referenced article, the value of 3.2 eV is that which he deduced for "the energy level of the dissociation limit" for ground-state fragments on the basis of his ion kinetic-energy measurements, the then accepted (but incorrect) value of D(NO), and the (false) assumption that the O^- ion was excited to a near-continuum state. Later reappraisal of his own data [H. D. Hagstrum, J. Chem. Phys. 23, 1178 (1955)], in the light of more accurate knowledge of the electron affinity of O and D(NO), gave the value 5.3 eV for the dissociation limit. A complete reinterpretation of the original data, properly taking into account the effects of the thermal motion of the target gas (see Ref. 1), would undoubtedly lead to a still higher value. As the present work shows, the dissociation limit and the observed appearance potential in fact coincide at 7.4 eV. Irrespective of all the above problems of interpreting data such as those of Hagstrum, there is clearly a basic discrepancy between the observed appearance potential (5.0 eV) of Hierl and Franklin, and that of Hagstrum and all other workers (7.0–7.5 eV).

[8]The theory presented in Ref. 2 (CS) assumed that both fragments are in their ground states. Eq. (4) above is an obvious extension of Eq. (3) in CS to the case where fragment Y is excited.

[9]Eq. (5) is essentially Eq. (A1) in CS, written in terms of the energy E, multiplied by the instrumental energy discrimination factor E^{-n}.

[10]Solutions to (5) include also any minima which may have been imposed on the true distribution by the E^{-n} weighting factor. The problem of solving (5) for multiple roots is avoided by solving for α_0 as a function of α, by iteration. See Fig. 1.

[11]This corresponds to the high energy limit of Eq. (7) when $\alpha_0{}^2 = \alpha_p{}^2 + 2n$.

[12]R. E. Fox, W. M. Hickam, D. J. Grove, and J. Kjeldaas, Rev. Sci. Instr. 26, 1101 (1955).

[13]It must be assumed that some of the ions formed near the entrance and exit plates of the collision chamber reach these plates rather than the attractor.

[14]With the present electrode geometry, the extraction field applied between the repeller and attractor produces planar equipotential surfaces in the region of the electron beam. Ideally one requires that the surface traversed by the beam be at the potential of the collision chamber box. In practice, it is found preferable to arrange that this surface be a few tenths of a volt negative with respect to the collision chamber, thereby ensuring that the electron beam is retarded in the volume of the collision chamber, in which case confidence may be placed in a retarding-curve calibration of the electron energy scale.

[15]R. E. Fox and W. M. Hickam, J. Chem. Phys. 22, 2059 (1954).

[16]This is exact for an idealized distribution of the form considered by R. K. Asundi and M. V. Kurepa [J. Sci. Instr. 40, 183 (1963)]. In principle the retarded distribution used in the present work has a sharply defined low-energy cutoff. In practice, imperfections in the retarding lens cause this cutoff to be somewhat smoothed. Thus the most probable energy occurs somewhere between the minimum energy and the average energy of the distribution. These are found to be separated by 0.2 eV, so that the error involved in equating the mean of them to the most probable energy cannot exceed 0.1 eV, and is probably much less.

[17]G. G. Cloutier and H. I. Schiff, J. Chem. Phys. 31, 793 (1959).

[18]R. E. Fox, W. M. Hickam, and T. Kjeldaas, Jr., Phys. Rev. 89, 555 (1953).

[19]The conclusion is valid provided the curve does not have a hump at larger internuclear separations (see Fig. 10).

[20]According to the theory in Sec. I, the position of the peak for $E_0 = 0$ is $\beta kT/2$, which for these cases ≈ 0.01 eV. Within the reproducibility of the scale, this may be taken as zero.

[21]Apart from their magnitudes, the cross sections in the threshold region appear to differ only with regard to the slope above threshold. In CO it is negative, in NO it is positive in this immediate region. Over the range of interest to the present discussion (a few tenths of an eV), both may be approximated by a step function. See Sec. III for a discussion of the exact shape of the cross section in NO in the threshold region.

[22]The factor $E_0{}^{-1/2}$ takes account of the variation with E_0 of the ratio of the peak height to area of the ion energy distribution [see Eq. (A1) of CS].

[23]Since the errors arising from this effect are very small, no systematic study of the factors controlling its variation from run to run has been made. It is known to be dependent on the choice made for the accelerating voltage applied to the accelerating grid between the collision chamber and the filter. As discussed above, this choice was controlled by other criteria.

[24]The difference ion current is that produced by the difference electron energy distribution provided by the R. P. D. technique.

[25]G. Herzberg, Mem. Soc. Roy. Sci. Liege 18, 397 (1957).

[26]L. M. Branscombe, D. S. Burch, S. J. Smith, and S. Geltman, Phys. Rev. 111, 504 (1958).

[27]The ion accelerating voltage increases from right to left on these plots. The scale shown is that corresponding to the initial ion kinetic energy.

[28]C. E. Moore, Natl. Bur. Std. (U.S.), No. 467, 1, 22 (1949).

[29]The reaction (9) has been previously identified by C. R. Lagergren, Ph. D. thesis, University of Minnesota, 1955 (unpublished), [Dissertation Abstr. 16, 770 (1956)] in mass-spectrometric work employing the

R. P. D. technique. The inherent preferential detection of low-energy ions by his instrument allowed the process to be observed as a second hump in the ionization efficiency curve for O^- production from CO. For a summary of Lagergren's data see M. A. Fineman and A. W. Petrocelli, J. Chem. Phys. 36, 25 (1962).

[30]This serves to rule out the possibility that the second peak arises from a two-step process in which the electron first loses 1.22 eV of energy and is then attached by the same mechanism as the first peak.

[31]This shift is within the accuracy of electron energy scale calibration claimed for either experiment.

[32]C. E. Moore, Ref. 28, p. 32.

[33]J. N. Bardsley, A. Herzenberg, and F. Mandl, in *Atomic Collision Processes*, edited by M. R. C. McDowell (North-Holland Publishing Co., Amsterdam, 1964), p. 415.

[34]T. F. O'Malley, Phys. Rev. 150, 14 (1966).

[35]J. C. Y. Chen and J. L. Peacher, Phys. Rev. 163, 103 (1967).

[36]The entrance width is the uncertainty in the energy of the intermediate XY^{-*} state associated with the probability that it decay by autodetachment back to the ground electronic state. It is a measure of the transition probability between these two states, and thus may be called the entrance width or partial decay width.

[37]The resonant nature of the capture process provides a one to one relationship between the internuclear separation R and the energy of the captured electron E, permitting both ρ and χ to be written as unique functions of E.

[38]See, for example, H. D. Hagstrum, Rev. Mod. Phys. 23, 185 (1951) and G. G. Cloutier and H. I. Schiff, J. Chem. Phys. 31, 793 (1959).

[39]In the case of O^- from O_2, the effect of higher initial vibrational and rotational states gives rise to a significant temperature dependence of the cross section. [See W. L. Fite, R. T. Brackmann and W. R. Henderson, *Proceedings of the Fourth International Conference on the Physics of Electronic and Atomic Collisions* (Science Bookcrafters, Inc., New York, 1965)].

[40]In the case of H^- production from H_2 and its isotopes, the variation with nuclear mass of the time during which autodetachment is possible gives rise to a strong isotope dependence of the magnitude of the cross section. [See G. J. Schulz and R. K. Asundi, Phys. Rev. 158, 25 (1967)].

[41]T. F. O'Malley, Phys. Rev. 155, 59 (1967).

[42]J. C. Y. Chen and J. L. Peacher, Phys. Rev. 167, 30 (1968).

[43]In the production of O^- from O_2, for example, this factor shifts the observed peak to lower energies by 1 eV at room temperature (see Ref. 41). Thus, the O_2^- potential energy curve derived from the reflection method is too low by 1 eV in the Franck-Condon region.

[44]The ground-state curve for CO has been taken from P. H. Krupenie and S. Weissman, J. Chem. Phys. 43, 1529 (1965). The neutral curves for NO have been taken from F. R. Gilmore, J. Quant. Specty. Radiative Transfer 5, 369 (1965).

[45]This latter conclusion must be regarded as tentative. A similarly shaped cross section is observed in H^- production from H_2 at low energies (see Ref. 40), to which the same reasoning might be applied, with the conclusion that the $^2\Sigma_u{}^+H_2{}^-$ curve crosses the dissociation limit at an internuclear separation somewhere in the region $R < R_e \simeq 1.45a_0$ where R_e is the equilibrium separation of H_2 ground state. However, the semiempirical curve derived by J. C. Y. Chen and J. L. Peacher [Phys. Rev. 167, 30 (1968)] from the dissociative attachment data of Ref. 40 lies above the dissociation limit for $R < 1.55a_0$. As one might expect, the peak in the Gaussian ground-state nuclear wave function then appears in the nuclear overlap integral [see Fig. 4 of J. C. Y. Chen and J. L. Peacher, Phys. Rev. 167, 30 (1968)]. This shape is, however, so strongly modified by the other energy dependent factors that the peak in the Gaussian ground-state nuclear wave function is not discernible in the final cross section. On the other hand, *ab initio* calculations of this H_2^- curve [I. Eliezer, H. S. Taylor, and J. K. Williams, Jr., J. Chem. Phys. 47, 2165 (1967)], place it below the dissociation limit throughout the Franck-Condon region, rising above it only at smaller internuclear separations, in the wing of the ground-state vibrational excitation. A more recent semiempirical curve [J. C. Y. Chen, *Advances in Radiation Chemistry* (John Wiley & Sons, Inc., New York, 1968), Vol. I] derived from vibrational excitation data has a similar form, as does the qualitative curve presented by G. J. Schulz and R. K. Asundi in Ref. 40.

[46]Evidence as to the number of NO^{-*} states involved in dissociative attachment could probably be obtained from measurements of the angular distribution of the O^- ions as a function of energy. See G. H. Dunn, Phys. Rev. Letters 8, 62 (1962).

[47]For example, a relatively sharp decrease in the survival probability as the electron energy is increased above approximately 8 eV could interrupt what would otherwise be a monotonically increasing cross section in this region of energy, thereby producing the first peak. The second peak may then be interpreted as being generated by the peak in the Gaussian ground-state vibrational wave function. Alternatively, the minimum may be associated with a local depression of the survival probability due to the NO^{-*} curve crossing the repulsive portion of an excited neutral state curve, as proposed to explain similar structure in H^- production from H_2 at 11.2 eV (I. Eliezer, H. S. Taylor, and J. K. Williams, Jr., Ref. 45). If the effect is of this type, the most likely neutral curve is the $G^2\Sigma^-$ state of NO. The wealth of neutral-state curves in this region (see Ref. 44) means that many such curve crossings undoubtedly occur, and it would not be surprising if the structure in the attachment cross section arises from local sharp changes in the survival probability.